Challenges in simulating coastal effects on an offshore wind farm

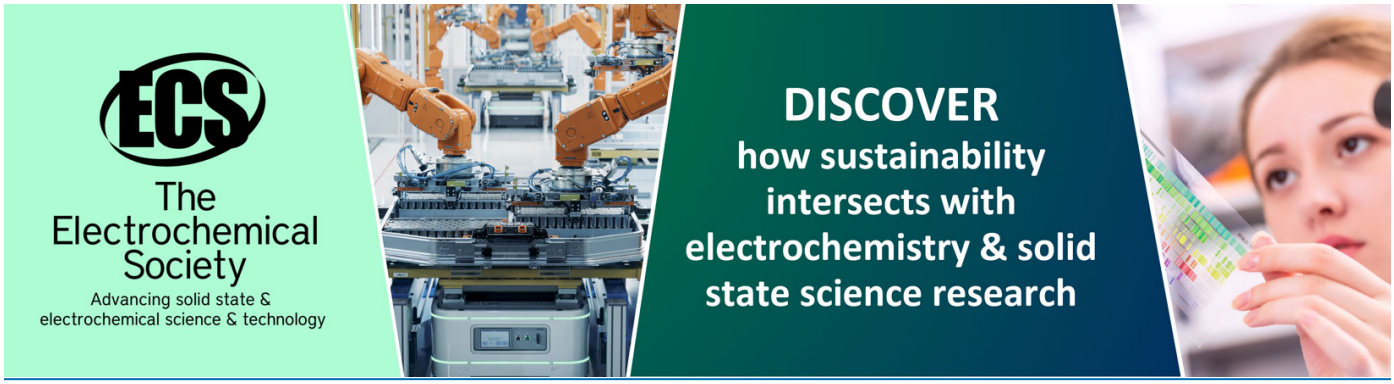

IOP Conf. Series: Journal of Physics: Conf. Series **854** (2017) 012046 doi:10.1088/1742-6596/854/1/012046

Challenges in simulating coastal effects on an offshore wind farm

M. P. van der Laan[1], A. Peña[1], P. Volker[1], K. S. Hansen[2], N. N. Sørensen[1], S. Ott[1], C. B. Hasager[1]

[1]Technical University of Denmark, DTU Wind Energy, Risø Campus, DK-4000 Roskilde, Denmark
[2]Technical University of Denmark, DTU Wind Energy, Lyngby Campus, DK-2800 Kgs. Lyngby, Denmark

E-mail: plaa@dtu.dk

Abstract. The effect of a coastline on an offshore wind farm is investigated with a Reynolds-averaged Navier-Stokes (RANS) model. The trends of the RANS model compare relatively well with results from a mesoscale model and measurements of wind turbine power. In addition, challenges of modeling a large domain in RANS are discussed.

1. Introduction

Wind turbine wakes can cause energy losses in wind farms [1] and their effect needs to be modeled in order to design energy efficient wind farm layouts [2]. Wake losses in offshore wind farms are often modeled by assuming offshore conditions for all wind directions [3, 4, 5, 6, 7]; however, many offshore wind farms are build in the vicinity of a coastline. Dörenkämper et al.[8] used Large Eddy Simulations (LES) of an offshore wind farm to show that a varying distance between the coast and a wind farm can have a large influence on the wind turbine power. In addition, coastal effects are clearly visible in measurements of wind turbine power (Supervisory Control and Data Acquisition [SCADA]) of the Danish Anholt offshore wind farm [9]. For westerly and south westerly winds, the distance from the coastline (Danish Peninsula Djursland) to the Anholt wind farm varies between 15 and 50 km. This causes a horizontal wind speed gradient that results in a variation of wind turbine power along the north-south oriented rows, which is clearly visible in the measurements.

The effect of wind turbine wakes can be modeled with different levels of model fidelity [10], ranging from simple engineering wake models up to high fidelity Computational Fluid Dynamics (CFD), e.g. LES. In previous work, we have shown that Reynolds-averaged Navier-Stokes (RANS) simulations of wind turbine wake interaction in a neutral atmospheric surface layer can predict power deficits that compare well with LES [11] and SCADA measurements [7], if a proper turbulence model is used [12]. In this study, we want to investigate if the effect of the Djursland coastline on the Anholt offshore wind farm can be modeled by a RANS setup. The main model challenge is how to model the inflow of the Anholt wind farm including the horizontal wind speed gradient. In the LES of Dörenkämper et al.[8] this model challenge was handled by selecting an inflow profile from a library of precursor simulations representing different distances to the coast. In the current article, we can afford to include the coastline in

a large flow domain and model it as a roughness change since the grid requirements of RANS are not as demanding as in LES of atmospheric flows. The resulting horizontal wind speed gradient from RANS is compared with mesoscale simulations of Djursland using the Weather, Research and Forecasting (WRF) Model without the Anholt wind farm [13]. In addition, the horizontal wind speed gradient derived from the SCADA measurements using the official power curve is also compared with RANS. Finally, the simulated power deficits from RANS (including the coastal effects) are validated with the SCADA measurements.

The Anholt offshore wind farm test case is presented in Section 2. The methodology of the RANS simulations are described in Section 3. The comparison of the RANS simulations with the mesoscale simulations and SCADA measurements is discussed in Section 4.

2. Test case

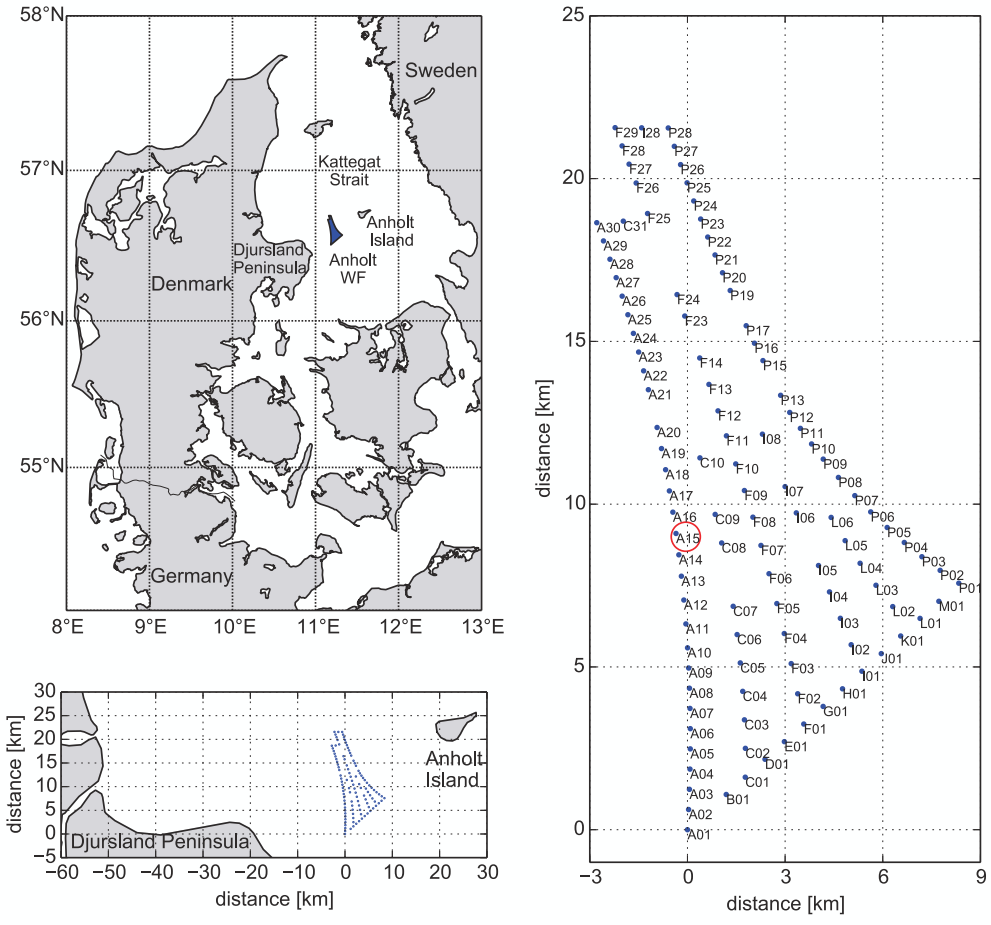

Figure 1. Location and layout of the Anholt offshore wind farm. Top left plot: Denmark, bottom left and right plots are zoomed views showing relative distances. Blue dots represent wind turbines. Red circle marks wind turbine A15 that is used as a reference wind turbine in Figures 6, 7 and 8.

The location and layout of the Anholt offshore wind farm is shown in Figure 1. The Anholt

wind farm is located in the Kattegat Strait, 15 km east of the Djursland Peninsula, and it fits in a rectangular box of 12 km by 22 km. Anholt consists of 111 Siemens 3.6 MW wind turbines with a rotor diameter and hub height of 120 and 81.6 m, respectively. The smallest distance between the wind turbines is 4.9 rotor diameters. For westerly wind directions, the distance from the Anholt wind farm to the coast varies between 15 and 50 km. In Figure 2, a wind rose at the middle of the Anholt wind farm is extracted from WRF simulations of Denmark [13], for the year 2014. The Anholt wind farm is affected by the wake of the Djursland Peninsula between 200-270°, which is about 30% of the wind rose. We are interested in a wind direction sector where the distance of the coast to the Anholt wind farm strongly varies for the north-south rows, i.e. 240-270°.

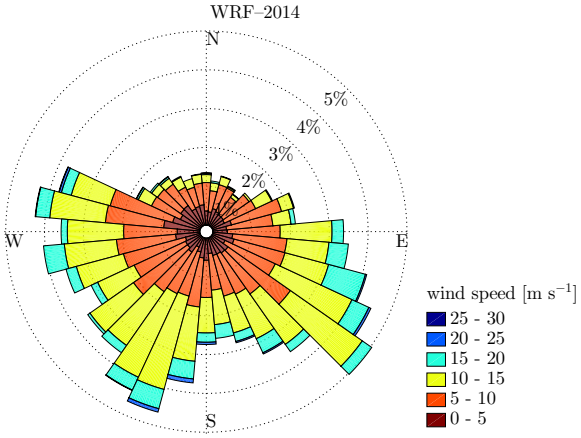

Figure 2. Wind rose of Anholt wind farm for the year 2014, simulated by WRF.

DONG Energy has provided raw SCADA measurements of all wind turbines, measured for 2.5 years between 2013-01-01 and 2015-07-01. The SCADA measurements are filtered for a wind speed bin of 9 ± 1 m/s, where the reference wind speed is determined from the power of a group of 4 wind turbines using the official power curve. For the wind direction sectors 230-270°, 270-280° and 280-310°, wind turbines A22-A25, A17-A20, A23-A26 are used to calculate the reference wind speed, respectively. The reference wind direction is determined from wind turbines A01, A16, A30, F29, P28 and P01 using yaw sensors that are calibrated with the peak deficit of neighboring wind turbines. One should keep in mind that it is difficult to obtain a global reference wind speed and wind direction for westerly wind directions because the inflow conditions vary in the north-south oriented rows. In addition, the SCADA measurements have been filtered for neutral and near-neutral atmospheric stability [14] using the WRF results.

3. Methodology

A brief description of the RANS setup is presented in this Section, while a full description can be found in previous work [15]. The RANS equations are solved in EllipSys3D, an incompressible flow solver developed at DTU Wind Energy [16, 17]. The turbulence is modeled by an alternative k-ε model that is suited to model wind turbines wakes (k-ε-f_P model [12]) and produces a finite boundary layer height by limiting the global turbulent length scale [18]. In addition, Coriolis forces are added to the momentum equations, which means that wind veer is also present in the flow domain. Only neutral atmospheric stability is considered. The effect of the coastline is modeled by roughness only and terrain heights are not modeled.

The numerical domain is plotted in Figure 3, where every 16th grid line is shown. The domain has a size of $300\times300\times0.9$ km^3 in x, y and z (height) direction, respectively. A green area is

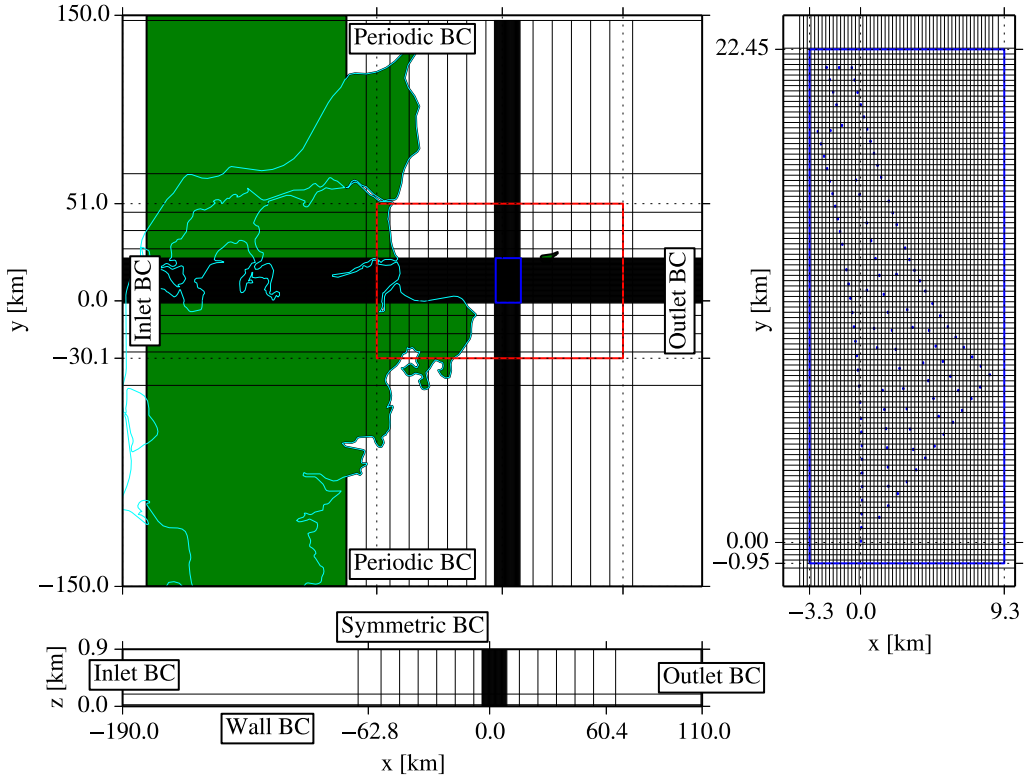

Figure 3. Grid, boundary conditions and roughness of wind farm simulations. Left top plot: top view, Left bottom plot: side view, right plot is a zoomed view of the left top plot. Every 16th grid line is plotted. Green area in left top plot indicates the modeled land with a roughness of 0.05 m, while cyan line indicates the real coastline. Red and blue boxes are regions with uniform horizontal spacing, blue squares in the right plot are actuator disks.

shown in the top left plot of Figure 3, which indicates where a land roughness is applied. Both the east coast of Denmark and the Anholt island are included. The land areas are modeled by a constant land roughness of 0.05 m, representing farmland with open appearances. The sea roughness is set to 10^{-4} m. The real coastline is plotted in the top left Figure 3 as a cyan line. The modeled land roughness deviates from the real roughness for two reasons. In order to use periodic conditions at the boundaries at $y = \pm 150$ km, the coastline is changed to a vertical line at $x = -78$ km for 120 km $<$ y $<$ -90 km. In addition, the land roughness area is 100 km extended upstream (in x direction), up to $x = -178$ km. A sea roughness is used in the first 12 km of domain such that the roughness at inlet boundary condition (BC) ($x = -190$ km) is in balance with the roughness at the outlet BC ($x = 110$ km), where fully developed conditions are assumed. If land roughness would be used at the inlet, the inlet Atmospheric Boundary Layer (ABL) profile based on land roughness would not develop to an ABL profile based on sea roughness (calculated by a precursor simulation based on sea roughness), after the roughness change, for $x \to \infty$, because of mass conservation. To illustrate this issue, a RANS simulation of a 100 km long domain has been carried out, where the first 20 km is land roughness and the remaining 80 km is based on sea roughness. The inlet profile is based on a precursor simulation with land roughness. In Figure 4, the ABL profiles at three downstream distances

are compared with the precursor profiles based on land and sea roughnesses. Figure 4 shows that the ABL profile from the inlet does not develop to the precursor profile based on the sea roughness because the total mass flow of the land profile does not match the total mass flow of sea profile.

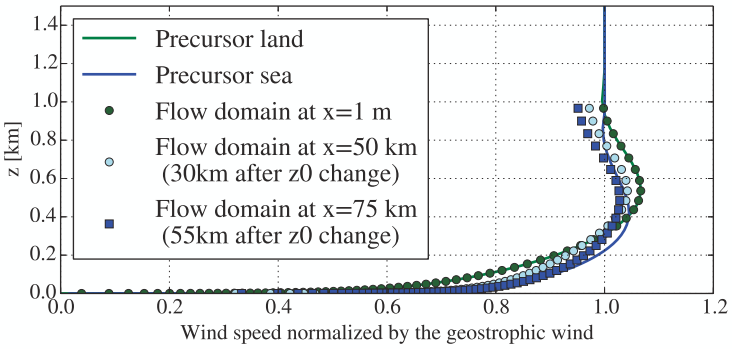

Figure 4. Downstream development of an ABL profile after a roughness change from land to sea using an inlet profile based on land that is not in balance with the sea roughness used at the outlet.

The inlet profiles that are applied to the inlet BC are calculated with a precursor simulation using a geostrophic wind of 10.5 m/s, the sea roughness (10^{-4} m), a Coriolis parameter of $f_c = 1.22 \times 10^{-4}$ 1/s (latitude of 56.6°) and a maximum turbulent length scale of $\ell_{t,\max} = 0.00027\frac{G}{f_c} = 23.3$ m, following Blackadar [19]. The results of the precursor simulation are shown in Figure 5, where the bottom figures are zoomed views of the top figures. Note that we do not use the additional max limiter on ε that we have used in previous work [15] to avoid an overshoot in the turbulent length scale because its effect is negligible. The other BCs in the numerical domain of Figure 3 are a wall boundary at $z = 0$ suited to satisfy a logarithmic profile [20] and a symmetric BC at the $z = 0.9$ km is applied. Ideally, one would prefer to use a taller domain height; however, the combination of the large domain with roughness changes and an ABL profile with low eddy viscosity above the ABL height ($z \approx 1$ km) can result in numerical instabilities. When a low domain height of 0.9 km is used, these numerical instabilities disappear.

In Figure 3, red and blue rectangles indicate regions where a uniform horizontal spacing of 600 m and 15 m is applied, respectively. Around the blue rectangle, the grid spacing grows outwards from 15 m to 600 m with a grow ratio of approximately 1.2. A spacing of 15 m, or $D/8$, is based on grid study of a single wind turbine wake [12]. The 600 m ($5D$) spacing is based on a grid study presented in Section 4.1. The total amount of cells is 120 million. Without modeling the coastline the total amount of cells would be around 100 million, which means that the coastline adds 20% of cells to the grid. The first cell height is set to 0.05 m.

The wind turbines are modeled as actuator disks [21] with variable forcing, where a fixed force distribution is scaled by the disk averaged velocity and a thrust coefficient that is function of the disk averaged velocity [11].

4. Results and Discussion

4.1. Wind farm inflow conditions and grid sensitivity study

Figure 6 shows the wind speed at row A calculated by RANS and WRF (both without the wind farm present in the simulations). The WRF data is binned in 10 degree bins at the location of wind turbine A15 and it is extracted from the same period as the SCADA measurements. The WRF data is filtered for neutral conditions, where only data points with a Monin Obukhov length larger than 500 m are kept. The Monin Obukhov length is calculated at the first cell

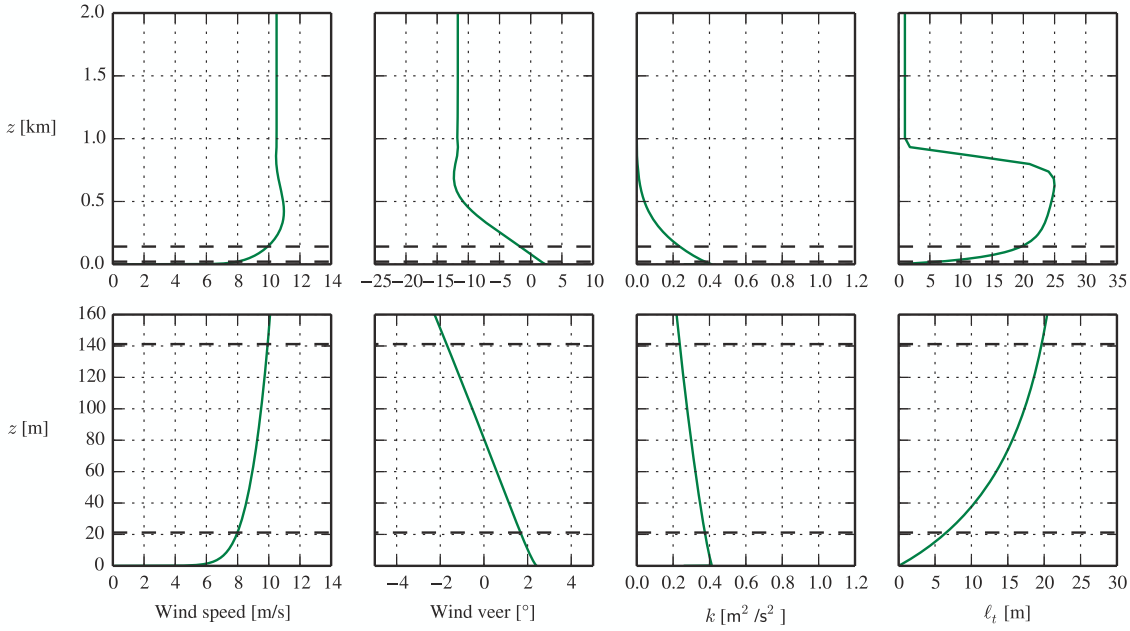

Figure 5. Inlet profiles calculated by the precursor and rotated for zero wind veer at hub height. Bottom plots are a zoomed view of the top plots. Rotor area is shown as black dashed lines.

located at 14 m. Note that the WRF data is not filtered for wind speed because the number of data points becomes too small if wind speed filtering is applied. The RANS results are made a follows. First a parametric run of 41 different freestream wind directions between 245° and 285° with an interval of 1° is carried out, without the wind farm present in the flow domain. Secondly, the wind direction at the location of wind turbine A15 is probed and it is used to bin all RANS simulations in 10° intervals from which a linear bin average is calculated. The re-binning is necessary because the freestream wind direction at the inlet changes downstream due to the interaction of two roughness changes with the Coriolis forces (sea $\rightarrow$ land $\rightarrow$ sea, while going from the inlet towards wind turbine A15). For example, the RANS simulation for a freestream wind direction of 285° calculates a wind direction of 281° at the location of wind turbine A15.

Three RANS results are shown in Figure 6 that are made by three different horizontal spacings in the red rectangle from Figure 3, namely 300 m, 600 m and 1200 m. Note that the finer spaced area in the blue rectangle from Figure 3 is not present in this grid sensitivity study. Figure 6 shows that there is only a small difference between a spacing of 1200 m and 600 m (mainly for the wind direction sectors $260° \pm 5°$ and $270° \pm 5°$), while there is no noticeable difference between a spacing of 600 m and 300 m. Therefore, a grid spacing of 600 m is sufficient to model the effect of the coastline.

The measured trends in the horizontal wind speed gradient are reasonably well captured by the RANS and WRF models, although there are differences. The observed mean wind speed gradient in the SCADA measurements is larger than those calculated by RANS and WRF for $250° \pm 5°$ and $260° \pm 5°$. For a wind direction of 275° and larger, the wake of Djursland does not affect the wind farm, which is observed as a nearly flat curve for the wind direction bin $280° \pm 5°$ in Figure 6, for the RANS results and the SCADA measurements (where a small

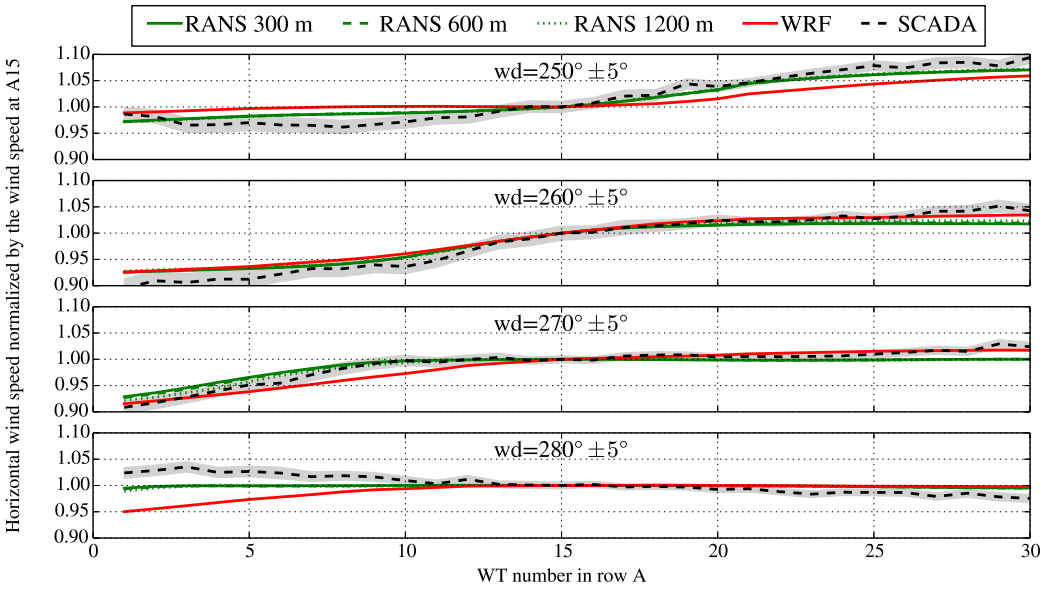

Figure 6. Wind speed at row A for westerly wind directions. RANS and WRF simulations are carried out without wind farm. The three RANS results are made with a horizontal spacing of 300 m, 600 m and 1200 m. The gray region around the SCADA measurements represents the uncertainty of the mean.

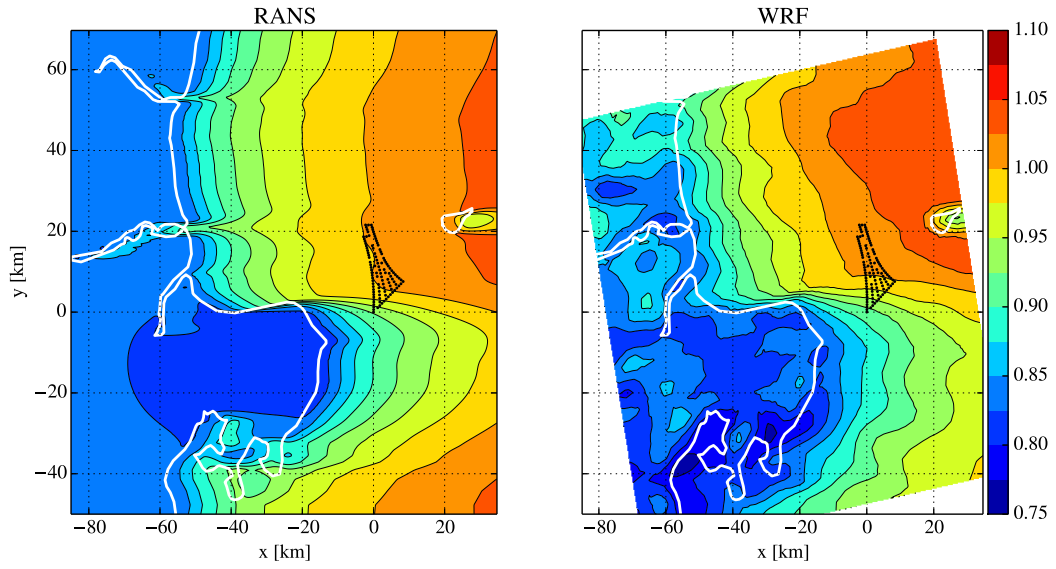

Figure 7. Contours of the horizontal wind speed at hub height for a wind direction of 270° ±5°, calculated by RANS and WRF. Coastlines and wind turbines are shown as a white line and black filled circles.

gradient is observed over the entire row A in the opposite direction). However, the WRF results still show a gradient for the same wind direction bin for wind turbines A1-A9. This indicates that the wake of Djursland is more wide spread in WRF compared to the RANS results and

SCADA measurements. The horizontal wind speed gradient of the other three wind direction bins from WRF show similar trends compared to RANS, although the gradients in WRF are shifted towards the south for $250^\circ \pm 5^\circ$ and $270^\circ \pm 5^\circ$.

Figure 7 depicts wind speed contours at hub height calculated by RANS and WRF, for the wind direction bin $270^\circ \pm 5^\circ$. The wind speed contours from WRF show a complex flow over land because a non uniform roughness is used. The speed up effects from the fjords is clearly visible in the RANS results, while is absent in the results from WRF, possibly because the WRF model is run with a horizontal resolution of 2 km. Overall, the comparison between RANS and WRF is difficult because RANS does not include any mesoscale effects (e.g. a varying geostrophic wind) and the WRF results are not filtered for wind speed.

4.2. Wake effects

Figure 8 shows a comparison of the wind farm simulation from RANS with the SCADA measurements, for 4 wind directions bins of 10°. The left two columns are contour plots of horizontal wind speed calculated by RANS. The right two columns are plots of wind turbine powers normalized by the power of wind turbine A15, where the most right plots are taken from the SCADA measurements. RANS simulation including the wind farm are carried out for every 5° between 230° and 290°, where the wind direction is measured at the location of wind turbine A15. The RANS results (both wind speed contours and powers) are Gaussian averaged with a standard deviation of 5° to represent the wind direction uncertainty in SCADA measurements [22]. Both the RANS results and SCADA measurements show a gradient in wind turbine power along the north-south rows that changes with wind direction. For the wind directions $250^\circ \pm 5^\circ$ and $260^\circ \pm 5^\circ$, the gradient in wind turbine power along the wind turbine rows A26-A30 and F25-F29 is stronger in the SCADA measurements compared to the RANS simulations, which is also visible in Figure 6. As a result, the downstream wind turbines of rows A26-A30 and F25-F29 also produce less power in the RANS simulations compared to the measurements. The wind turbine power from RANS compares well with the SCADA measurements for the other two wind direction bins $270^\circ \pm 5^\circ$ and $280^\circ \pm 5^\circ$, where the influence of Djursland Peninsula is small. While we have shown that RANS setup can model the effect of a coastline on a offshore wind farm, the comparison of the RANS results with the SCADA measurements could be improved by changing the input parameters of the RANS simulations, such as the roughness length of the coastline and the maximum turbulent length scale. A higher roughness of the coastline would increase the horizontal wind speed gradient in the RANS simulations. Setting a lower maximum turbulent length scale (ignoring the relation of Blackadar [19]) would result in a lower ABL height, a reduced eddy viscosity, and a higher wind shear and wind veer, that could affect the magnitude of the horizontal wind speed gradient.

4.3. Model challenges in RANS

In the current RANS setup, it is not possible to use a numerical domain with a height taller than 0.9 km due to numerical instabilities, as described in Section 3. Above the ABL height, a layer of low eddy viscosity exists, which can create numerical waves if the domain is tall enough to include this layer (> 0.9 km) and large enough in the horizontal dimensions. This problem needs to be solved because wind turbines wakes can be affected by the symmetric BC at the top of the domain if the domain height is shallow compared to the rotor diameter. One could possibly damp the fluctuations in the W velocity component with a source term in the W-momentum equation that is only active in the region above the ABL height.

5. Conclusions

A horizontal wind speed gradient along the north-south rows is observed in SCADA measurements of the Anholt wind farm for western wind directions. The wind speed gradient is

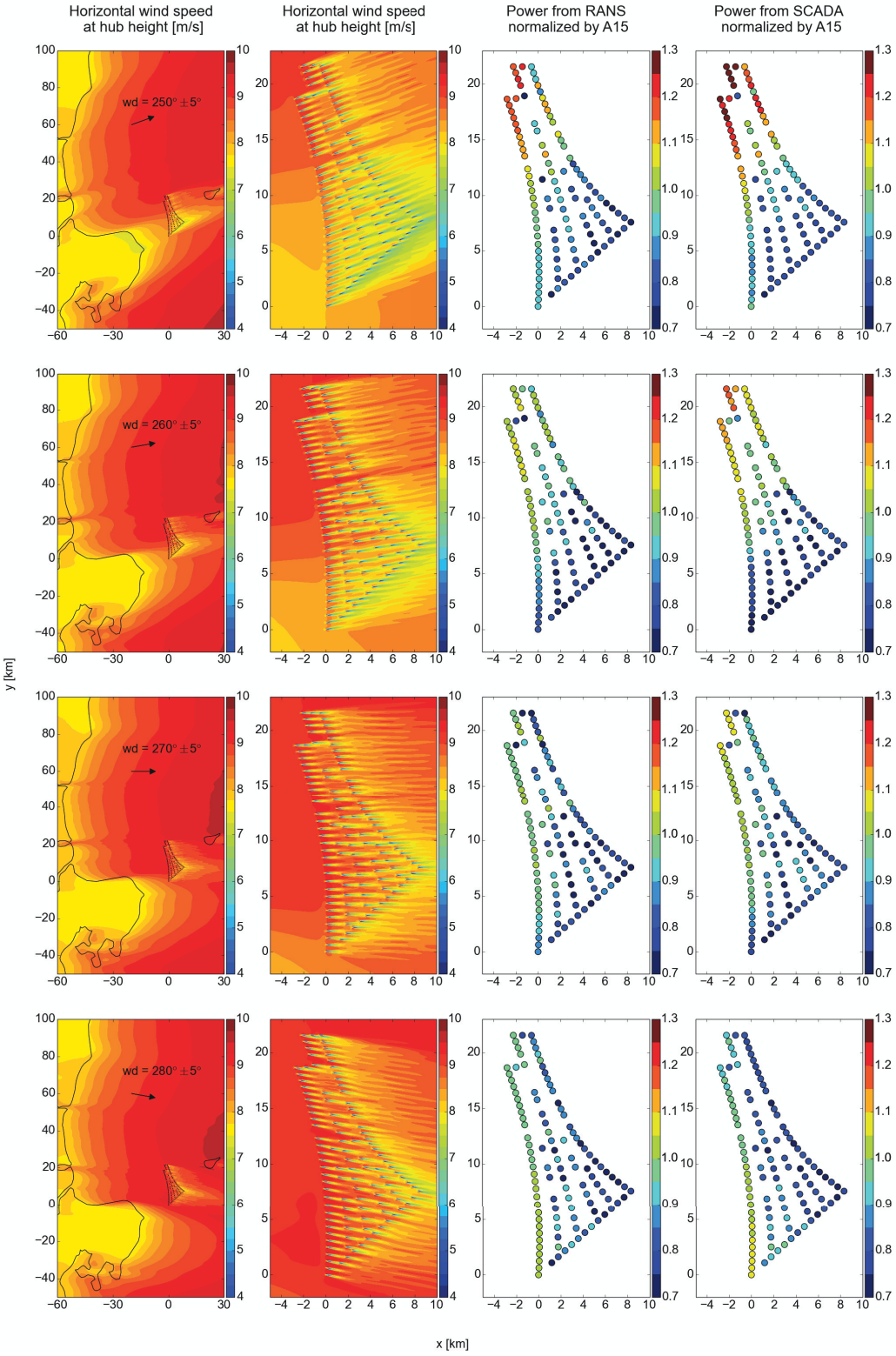

Figure 8. Contours of horizontal wind speed at hub height and normalized wind turbine power, for a wind direction of $250 - 280° \pm 5°$, calculated by RANS and observed in SCADA measurements. Coastlines and wind turbines are shown as a black line and black filled circles, respectively.

caused by a varying distance of the coastline to the wind turbines. The effect of the coastline on the Anholt offshore wind farm is investigated by a RANS model that can simulate wind turbines wakes in a neutral ABL including Coriolis forces. The trends of the horizontal wind speed gradient at the wind farm is reasonably well captured by the RANS model compared to a WRF model and the SCADA measurements. The RANS modeled effect of the coastline on the wind turbines wakes and corresponding power deficits shows similar trends as the SCADA measurements, although a higher gradient in wind turbine power along the north-south rows is observed for the wind direction sectors $250° \pm 5°$ and $260° \pm 5°$. The comparison could be improved by changing the input parameters of the RANS simulations. Overall, we shown that the RANS setup can model the effect of the coastline on the Anholt offshore wind farm.

The results from the RANS model are obtained using a large domain of 300×300 km^2, with a relative low domain height of 0.9 km. It is preferred to use taller domains; however, numerical instabilities are observed for taller domains due to the low eddy viscosity region above the ABL height. This problem needs to be solved in order to improve the RANS setup.

Acknowledgments
We would like to thank DONG Energy and partners for providing the SCADA measurements.

References
[1] Barthelmie R J, Frandsen S T, Nielsen N M, Pryor S C, Réthoré P E and Jørgensen H E 2007 *Wind Energy* **10** 217
[2] King R N, Hamlington P E, P G and Dykes K 2016 *American Institute of Aeronautics and Astronautics, 34th Wind Energy Symposium* 2016-2199
[3] Churchfield M J, Lee S, Moriarty P J, Martinez L A, Leonardi S, Vijayakumar G and Brasseur J G 2012 *AIAA conference 2012, Nashville, USA*
[4] Storey R C, Norris S E, Stol K A and Cater J E 2013 *Wind Energy* **16** 845
[5] Porté-Agel F, Wu Y T and Chen C H 2013 *Energies* **6** 5297
[6] Nilsson K, Ivanell S, Hansen K S, Mikkelsen R, Sørensen J N, Breton S P and Henningson D 2015 *Wind Energy* **18** 499
[7] van der Laan M P, Sørensen N N, Réthoré P E, Mann J, Kelly M C, Troldborg N, Hansen K S and Murcia J P 2015 *Wind Energy* **18** 2065
[8] Dörenkämper M, Witha B, Steinfeld G, Heinemann D and Khn M 2015 *Journal of Wind Engineering and Industrial Aerodynamics* **144** 146–153
[9] Damgaard S 2015 Open issues in wake model validation `http://www.windpower.org/download/2639/08_open_issues_in_wake_model_validationpdf` Vindkraftnet meeting on wakes
[10] Göçmen T, van der Laan M P, Réthoré P E, Peña Diaz A, Larsen G C and Ott S 2016 *Renewable and Sustainable Energy Reviews* **60** 752
[11] van der Laan M P, Sørensen N N, Réthoré P E, Mann J, Kelly M C and Troldborg N 2015 *Wind Energy* **18** 2223
[12] van der Laan M P, Sørensen N N, Réthoré P E, Mann J, Kelly M C, Troldborg N, Schepers J G and Machefaux E 2015 *Wind Energy* **18** 889
[13] Peña A and Hahmann A N 2017 30-year mesoscale model simulations for the noise from wind turbines and risk of cardiovascular disease project Tech. Rep. DTU Wind Energy-E-Report-0055(EN) DTU Wind Energy
[14] Hansen K S, Barthelmie R J, Jensen L E and Sommer A 2012 *Wind Energy* **15** 183
[15] van der Laan M P, Hansen K S, Sørensen N N and Réthoré P E 2015 *Journal of Physics: Conference Series* **524** 1
[16] Sørensen N N 1994 *General purpose flow solver applied to flow over hills* Ph.D. thesis DTU
[17] Michelsen J A 1992 Basis3d - a platform for development of multiblock PDE solvers. Tech. rep. DTU
[18] Apsley D D and Castro I P 1997 *Boundary-Layer Meteorology* **83** 75
[19] Blackadar A K 1962 *Journal of Geophysical Research* **67** 3095
[20] Sørensen N N, Bechmann A, Johansen J, Myllerup L, Botha P, Vinther S and Nielsen B S 2007 *Journal of Physics: Conference series* **75** 1
[21] Mikkelsen R 2003 *Actuator Disc Methods Applied to Wind Turbines* Ph.D. thesis DTU
[22] Gaumond M, Réthoré P E, Ott S, Peña A, Bechmann A and Hansen K S 2014 *Wind Energy* **17** 1169